

## Mechanical Instability of $\alpha$ -Quartz: A Molecular-Dynamics Study

John S. Tse and Dennis D. Klug

*Steacie Institute for Molecular Sciences, National Research Council of Canada, Ottawa, Ontario, Canada K1A 0R6*  
(Received 1 August 1991)

Pressure-induced amorphization in  $\alpha$ -quartz has been investigated using constant-pressure molecular-dynamics calculations with the two-body potential of van Beest, Kramer, and van Santen. Both the static properties and the crystalline-to-amorphous phase transition were very well reproduced. Through an analysis of the elastic moduli, the mechanism for the transformation is shown to be a mechanical instability driven mainly by a cooperative twisting and compression of the helical tetrahedral silicate units with an abrupt decrease in the  $C_{12}$ ,  $C_{23}$ ,  $C_{13}$ ,  $C_{14}$ , and  $C_{33}$  elastic moduli.

PACS numbers: 61.50.Ks, 64.60.Cn, 81.30.Hd

The study of transformations of crystalline materials to amorphous phases by the application of pressure is an important subject relating to the fundamental understanding of structural stability and the interrelationship between solid-phase equilibria. Many examples of these transformations have been discovered in the last several years [1-4] and show interesting and unusual features such as the ability to remain in the high-density amorphous phase after removal of pressure or memory effects where the pressurized phases can revert to their original structures. The understanding of these transformations at a molecular or atomic level is lacking. Several conflicting proposals have been suggested for the mechanism of these transformations. The original proposal by Mishima, Calvert, and Whalley [1] for ice is that a melting transition has occurred when the pressure exceeded the pressure on the extrapolated melting curve of the solid and the ice sample in effect "melts" to a high-density amorphous solid at 1 GPa at 77 K. A similar argument was proposed for  $\alpha$ -quartz by Hemley *et al.* [2] where they used a hypothetical extension of the melting curve of  $\alpha$ -quartz which suggested that the melting should occur at 20 GPa at 300 K. Melting is a qualitative concept. Thermodynamics requires equal free energies of the crystal and the liquid phase but this condition will not lead to information on the mechanism for the transition. The possibility of mechanical instabilities driving the crystal-to-amorphous transition in  $\alpha$ -quartz has been suggested [2]. The origin of this instability is not known, but a conjecture is that under severe compression, the O-O distances become so short that the crystalline structure is no longer stable [5]. No satisfactory microscopic theory for this novel transformation process has been substantiated. In this Letter, we report new results on the investigation of the mechanism for the crystal-to-amorphous solid-phase transition in  $\alpha$ -quartz which includes a detailed analysis of the changes in the structures and, in particular, the dynamical aspects were studied through the phase transition with the molecular-dynamics technique.

Molecular dynamics (MD) is a computational method of probing the mechanical and dynamical properties of crystals at the atomic level and is therefore capable of revealing the details of phase transformations providing

realistic interatomic potentials are available. In the case of  $\alpha$ -quartz, several effective potentials have been proposed. The potential used here is the two-body model derived by van Beest, Kramer, and van Santen [6] (BKS) which was constructed on the basis of a combination of *ab initio* calculations on a hypothetical  $H_4SiO_4$  cluster and fitting with the bulk properties. As will be reported elsewhere [7], this potential yields reasonable structures and dynamical properties for several polymorphs of silica at ambient and high pressures. More significantly, the BKS potential has corrected for the deficiencies of another two-body potential proposed by Tsuneyuki *et al.* [7,8].

The Nosé isothermal-isobaric MD method used here has been previously described in detail [9,10]. A model system consisting of 192  $SiO_2$  molecules was used in the calculations. The initial positions of the atoms were taken from the crystallographic data. Long-range electrostatic interactions were handled with the Ewald method [11]. In a typical MD run, time steps of 1-2 fs were used. At each pressure, the system was equilibrated with the temperature at 300 K for about 5000 time steps. The elastic constants were then calculated within the  $(N, p, H)$  ensemble from the fluctuations of the strain [12]. They were related to the adiabatic compliances and converted to elastic moduli through the appropriate transformations [11,13]. The elastic-constant calculations are fairly time consuming and usually require  $5 \times 10^4$  time steps. Close to the phase transition, even longer,  $10 \times 10^4$  steps with a time step of 0.8 fs, was taken in order to obtain full equilibration of the crystal before the transformation.

The main question addressed by this study is that of the mechanism for the crystal-to-amorphous phase transformation. According to the well-known Born stability criterion [13], the determinant of the coefficient matrix for the elastic moduli has to be nonsingular for a stable solid. This restriction for a trigonal crystal translates into the following conditions:

$$C_{11} - |C_{12}| > 0, \quad (C_{11} + C_{12})C_{33} - 2C_{13}^2 > 0, \\ (C_{11} - C_{12})C_{44} - 2C_{14}^2 > 0.$$

Therefore, monitoring the changes in the stability conditions will provide important information on the mechanism for the transition.

The volume and total energy versus pressure curves for  $\alpha$ -quartz are shown in Fig. 1. It clearly shows a sharp phase transformation occurring at 22.3 GPa with a volume reduction of  $2.79 \text{ cm}^{-3} \text{ mol}^{-1}$  or a densification of 16%. There is no precise experimental measurement on the transition pressure, but the transformation is observed to occur at 25–30 GPa [2]. The high-pressure phase is disordered as indicated by the atomic radial distribution functions and calculated structure factors. Further compression does not show any discontinuous change in the volume up to 80 GPa although the oxygen coordination number about a silicon atom increases from about five, immediately after the transition, to six at 80 GPa. X-ray diffraction studies on the transformed high-density phase show the structure is noncrystalline. There is some preliminary experimental evidence suggesting that the disordered phase may convert into six-coordinate stishovite above 60 GPa [14]. The calculated  $c/a$  ratio increases linearly from 1.10 at ambient pressure to 1.185 at 22 GPa [7], with  $a$  decreasing faster than  $c$  indicating that the crystal is stiffer in the  $c$  direction. This result is in good agreement with experiment [15] and is a sig-

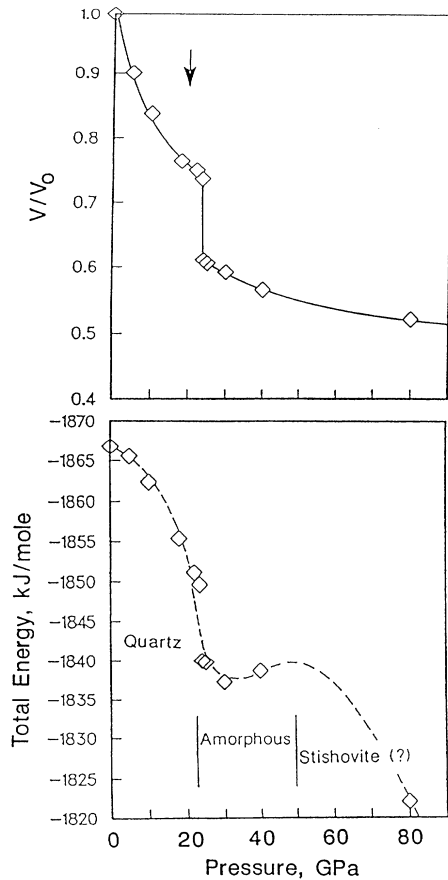


FIG. 1. The calculated (upper) volume change and (lower) total energy vs pressure for  $\alpha$ -quartz.  $V_0$  is the volume at ambient pressure.

nificant improvement over previously suggested potentials in this respect [16].

The elastic constants calculated at ambient pressure are (in Mbar)  $C_{11}=0.864$  (0.868),  $C_{33}=0.928$  (1.058),  $C_{44}=0.430$  (0.582),  $C_{66}=0.440$  (0.399),  $C_{12}=-0.024$  (0.070),  $C_{13}=0.040$  (0.191), and  $C_{14}=-0.171$  (-0.180), where the numbers in parentheses are the experimental values [17]. The results are in good agreement with experiment in view of the simplicity of the rigid-ion model. At 22.3 GPa, the crystalline phase was found to be stable in the first  $2.2 \times 10^4$  time steps (17.6 ps), and then a sudden densification occurs. These structural changes are signified by a sharp drop in the  $C_{33}$ ,  $C_{12}$ ,  $C_{23}$ ,  $C_{13}$ , and  $C_{14}$  moduli. In contrast, the  $C_{44}$ ,  $C_{55}$ , and  $C_{66}$  moduli increase at the transition while  $C_{11}$

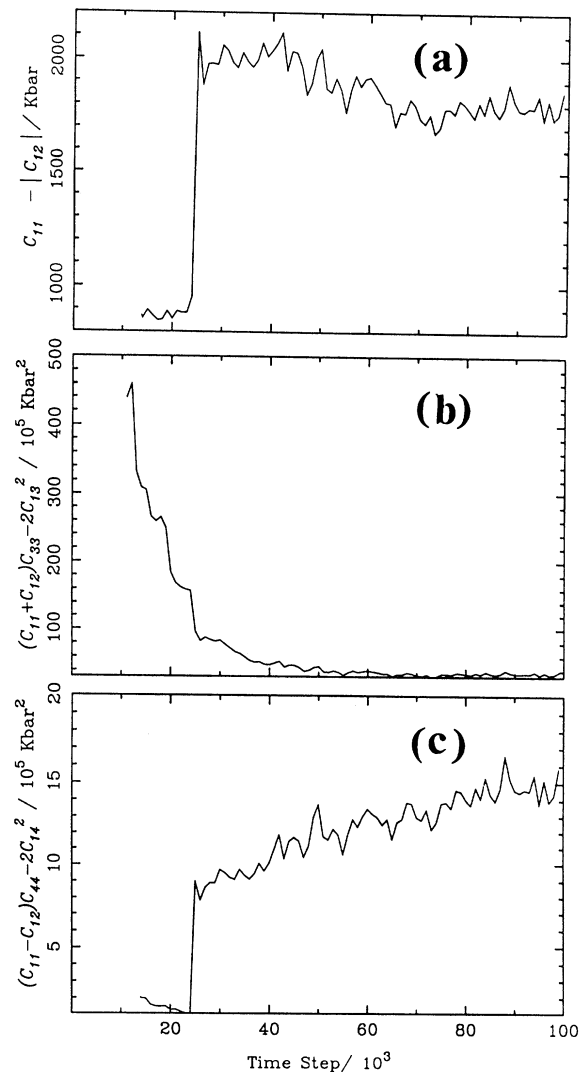


FIG. 2. The calculated temporal evolution of the Born stability conditions (a)  $C_{11} - |C_{12}|$ , (b)  $(C_{11} + C_{12})C_{33} - 2C_{13}^2$ , and (c)  $(C_{11} - C_{12})C_{44} - 2C_{14}^2$  for  $\alpha$ -quartz at 22.3 GPa. 1 time step = 0.8 fs.

remains essentially constant.

An examination of the Born criteria (Fig. 2) shows that the stability condition  $(C_{11} + C_{12})C_{33} - 2C_{13}^2 > 0$  has been violated when the crystal collapses into the high-density disordered phase. The sudden decrease in the  $C_{33}$  and the smaller  $C_{12}$ ,  $C_{23}$ , and  $C_{13}$  moduli indicate the strain in the crystallographic  $c$  direction has grown substantially. This can be explained whereby the helical silicate tetrahedra spiraling about the  $c$  axis are twisted (or tilted) and compressed simultaneously in order to relieve the stress. The cooperative twisting and compressive motions (supra, infra) soften the  $C_{33}$ ,  $C_{12}$ ,  $C_{23}$ ,  $C_{13}$ , and  $C_{14}$  elastic moduli. The big change in  $C_{33}$  appears to be the dominant factor since it changes faster than  $2C_{13}^2$  and  $C_{12}$  is smaller than  $C_{11}$  during the temporal evolution of the stability criterion. The increase in  $C_{11} - |C_{12}|$  is due to the rapid decrease in  $C_{12}$  and the increase in  $(C_{11} - C_{12})C_{44} - 2C_{14}^2$  is mainly due to the increase in  $C_{44}$ .

The bond angle distributions as a function of pressure are compared with experiment [18] in Fig. 3. The calculated pressure dependences of the O-Si-O and Si-O-Si angle distributions are in good agreement with experiment except that the calculated Si-O-Si values are higher by  $5^\circ$ – $6^\circ$ . It is particularly noteworthy that the BKS potential yields such a good description of these bond angle variations which was not achieved with the use of the other two-body potential [5]. Since the crystal structure is stable up to the phase transition, the local twofold symmetry at the Si atom is maintained. Thus, the six O-Si-O angles fall into four inequivalent sets. The results in Fig. 3 show that as the pressure increases, two sets of the O-Si-O angles open up accompanying the closing of the other two sets. This observation indicates a compression of the  $\text{SiO}_4$  tetrahedra. The opening of some O-Si-O angles allows oxygen atoms to fill the voids. This is reflected by the calculated increasing coordination number around the silicon atoms when the oxygen atoms are forced into the interstitial space through a rotation. As a consequence, the nearest-neighbor O-O distances also decrease as a result of the compressed Si-O-Si angles [5]. In effect, the  $\text{SiO}_4$  tetrahedra penetrate one another. A projection of the  $\text{SiO}_4$  tetrahedra down the  $c$  axis at 0 and 22 GPa (Fig. 4) clearly shows that tetrahedra were rotated and flattened under pressure. The pretransition structural changes involving simultaneous rotation and distortion of the  $\text{SiO}_4$  helical spiral shown in Fig. 4 are in remarkably good agreement with those derived from crystallographic studies [15] and a recent electronic structure calculation [5]. The MD calculation supports the notion that the onset of the phase transition is caused by an almost close packing of oxygen atoms with the nominal Si-O-Si angles approaching  $120^\circ$ . The interpenetration of the  $\text{SiO}_4$  tetrahedra clearly leads to a mechanical instability.

Other than the mechanical instabilities discussed above there are generally assumed to be two basic models for thermal melting of crystals which may be relevant to the discussion here. The Lindemann picture [19] can be dis-

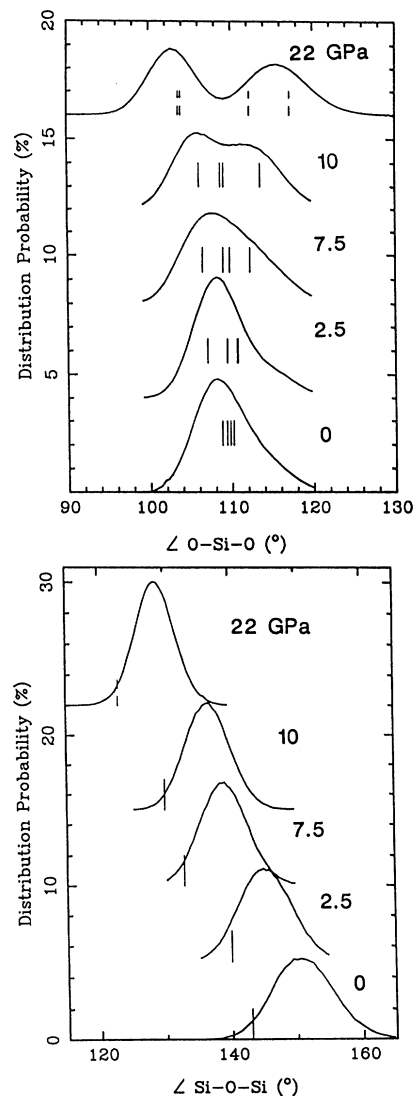


FIG. 3. Upper: The O-Si-O angles in  $\alpha$ -quartz as a function of pressure. The solid vertical lines are the experimental values and the dashed vertical lines are from an electronic calculation. Lower: The calculated and experimental Si-O-Si angles in  $\alpha$ -quartz as a function of pressure. The notation is the same as in the upper frame.

carded since there is no evidence that the atomic displacements increase with pressure. Another possibility is that the spontaneous generation of a large number of defects or dislocations causes the lattice to collapse [20]. This possibility is not consistent with the abruptness of the calculated transition. In the calculations no defects were observed before the phase transition. In contrast, the growth of defects is normally greatly hindered by increasing the pressure at low temperatures. Experimentally the transition is found to occur over a pressure range which may be due to pressure gradients which are not considered in the calculations.

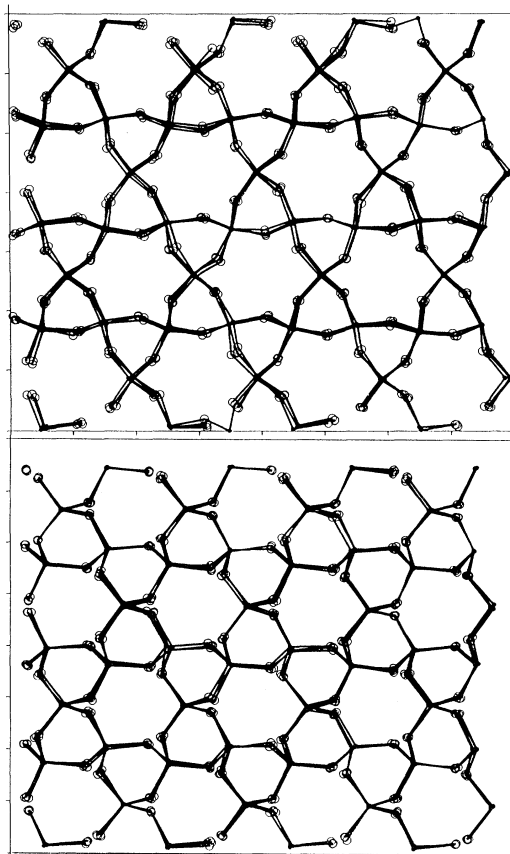


FIG. 4. The projection down the  $c$  axis for quartz at (upper) 0 GPa and (lower) 22 GPa. The open circles are oxygen atoms and the solid circles are silicon atoms.

In summary, it has been shown for the first time that the mechanism for the crystal-to-amorphous transition can be examined using constant-pressure molecular-dynamics methods. In particular, by following the temporal evolution of the elastic moduli as a function of pressure it can be shown that the driving force for this transition is a mechanical instability in the crystal. It is analogous to a mechanical melting [21]. The MD method has the ability to provide unique insight into this interesting class of solid-solid phase transitions at the atomic level and will be potentially useful for testing and extending our understanding of melting phenomena. In passing, the mechanism suggested for the pressure-induced phase transformation in  $\alpha$ -quartz may also be valid for  $\alpha$ -AlPO<sub>4</sub>

(Ref. [3]). We speculate, in the latter case, that the twisting and compression of both the aluminate and phosphate tetrahedra lead to a similar order-to-disorder transformation. Since the phosphate tetrahedra are strongly covalently bonded, the distortion in the local geometry is expected to be less significant. As a result, the transformed phase reverts into the crystalline form once the pressure is removed.

- 
- [1] O. Mishima, L. D. Calvert, and E. Whalley, *Nature* (London) **310**, 393 (1984).
  - [2] R. J. Hemley, A. P. Jephcoat, H. K. Mao, L. C. Ming, and M. H. Manghnani, *Nature* (London) **334**, 52 (1988).
  - [3] M. B. Kruger and R. Jeanloz, *Science* **249**, 647 (1990).
  - [4] J. S. Tse, D. D. Klug, and J. A. Ripmeester (to be published).
  - [5] J. R. Chelikowsky, H. E. King, Jr., N. Troullier, J. L. Martins, and J. Glinnemann, *Phys. Rev. Lett.* **65**, 3309 (1990).
  - [6] B. W. H. van Beest, G. J. Kramer, and R. A. van Santen, *Phys. Rev. Lett.* **64**, 1955 (1990).
  - [7] J. S. Tse and D. D. Klug, *J. Chem. Phys.* (to be published).
  - [8] S. Tsuneyuki, M. Tsukada, A. Aoki, and Y. Matsui, *Phys. Rev. Lett.* **61**, 869 (1988).
  - [9] S. Nosé, *J. Chem. Phys.* **81**, 511 (1984).
  - [10] S. Nosé and M. L. Klein, *Mol. Phys.* **50**, 1055 (1983).
  - [11] P. Ewald, *Ann. Phys. (Leipzig)* **64**, 253 (1921).
  - [12] M. Sprik, R. W. Impey, and M. L. Klein, *Phys. Rev. B* **29**, 4346 (1984).
  - [13] M. Born and K. Huang, *Dynamical Theory of Crystal Lattices* (Oxford Univ. Press, London, 1954), p. 148; F. I. Fedorov, *Theory of Elastic Waves in Crystals* (Plenum, New York, 1968), p. 33.
  - [14] Y. Tsuchida and T. Yagi, *Nature* (London) **347**, 267 (1990).
  - [15] R. M. Hazen, L. W. Finger, R. J. Hemley, and H. K. Mao, *Solid State Commun.* **72**, 507 (1989); J. D. Jorgensen, *J. Appl. Phys.* **49**, 5473 (1978).
  - [16] J. R. Chelikowsky, H. E. King, Jr., and J. Glinnemann, *Phys. Rev. B* **41**, 10866 (1990).
  - [17] J. Meskmin, P. Andreatch, and R. N. Thurston, *J. Appl. Phys.* **36**, 1624 (1965).
  - [18] L. Levien, C. T. Prewitt, and D. J. Weidner, *Am. Mineral.* **65**, 920 (1980).
  - [19] F. A. Lindemann, *Z. Phys.* **11**, 609 (1910).
  - [20] R. W. Cahn and W. L. Johnson, *J. Mater. Res.* **1**, 724 (1986).
  - [21] D. Wolf, P. R. Okamoto, S. Yip, J. F. Lutsko, and M. Kluge, *J. Mater. Res.* **5**, 286 (1990).